Preliminary Results on Comparison of LM Radiation Code to the LbL Model RTX

A. Bozzo

University of Bologna, ADGB, Bologna, Italy

1 Introduction and Model Description

The LM fast radiation scheme (Ritter and Geleyn, 1992) has been compared with the LbL-multiple scattering model RTX, that has been improved and extended during the last 5 years at ADGB (Atmospheric Dynamic Group – Dep. of Physics, University of Bologna). Motivation of the comparison is testing the accuracy of LM radiation code using RTX computations as benchmark. Main interest is checking the optical properties of gases and clouds, as modeled in LM.

RTX spectroscopic database is based on the modern HITRAN2000 and extends from far infrared (FIR) to 0.4 μm. We are working in order to extend the gaseous optical database up to the UV bands. Single scattering properties of water clouds are computed with exact Mie theory calculations. Optical properties of ice clouds are based on the most advanced parameterizations for aggregate and columns, made available to ADGB in a long standing cooperation with the Met Office. Adding and doubling method provide exact radiative transfer calculations in multiple scattering environments.

The LM radiative transfer code (named GRAALS, General Radiative Algorithm Adapted to Linear-type Solutions) is a fast delta-two stream radiation code with treatment of partial cloudiness via maximum-random overlap method. The optical properties of clouds and gases are parameterized over 8 wide spectral intervals from visible (VIS, 0.2 μm) to far infrared (FIR, 104.5 μm). Parameterizations by Slingo-Schrecker (1982) and Rockel (1991) is adopted for the computation of water and ice clouds single scattering properties respectively. The spectroscopic gaseous properties are based on the old AFGL '84 database.

In this work we will present the very first comparisons between the two models in some simple atmospheric situations. The basic settings of both the models concern a Lambertian surface and the gaseous absorption of the major atmospheric gases as CO_2, H_2O, O_3, N_2O, O_2, CO, CH_4 for both models. RTX consider also trace gases as CFCs (F11,F12,CCl4), NO, NO_2, SO_2, N_2. Monocromatic RTX fluxes are grouped in 7 of the 8 LM-GRAALS bands (the LM VIS range 0.2 μm - 0.7 μm is not taken in account due to the (for now) limited RTX solar spectroscopic database).

2 Comparisons

The first comparison scenario is a clear Standard tropical atmosphere (McClatchey et al, 1971). In Fig. 1 the thermal IR net fluxes show good agreement in terms of the shapes of the curves, but a bias affect the absolute values. In Fig. 2 the IR net flux is splitted in the contributions of the 5 thermal IR LM-GRAALS bands (i.e. contributions of the major gases). All curves show discrepancies between RTX and LM-GRAALS. In particular, the CO_2 bands show considerable higher LM-GRAALS net fluxes throughout the whole profile.

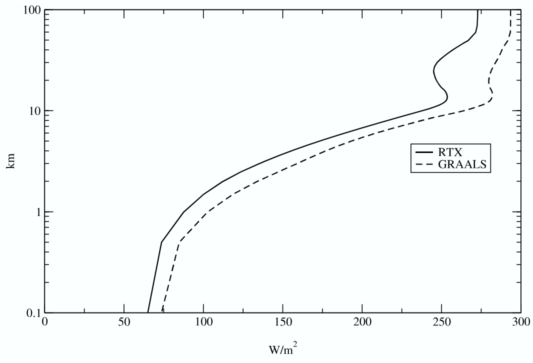

Figure 1: Thermal-IR (104-4.6 μm) Net Flux; (STD Trop. Atm. Profile – Sun zenith angle = 0°)

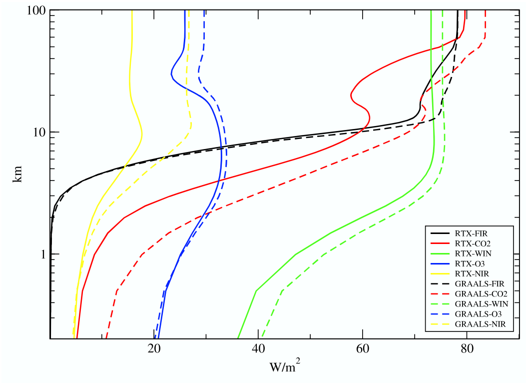

Figure 2: Thermal-IR (104-4.6 μm) Spectral Net Fluxes; (STD Trop. Atm. Profile – Sun zenith angle = 0°)

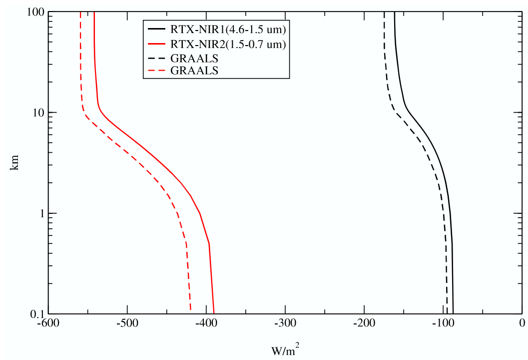

Figure 3: Solar-IR Spectral Net Fluxes; (STD Trop. Atm. Profile – Sun zenith angle = 0°)

Moreover the net fluxes diverge in the O_3 band in the layer where the maximum absorption is located, i.e. in the first stratospheric layers. The large discrepancy in the near infrared band (NIR) is due to the fact that the sun irradiance is distributed in LM_GRAALS only in the 3 solar bands (i.e. from 0.2 μm to 4.5 μm) instead to be treated as a continue spectral distribution as RTX do: the integral of the down-welling solar irradiance in the spectral range covered by the NIR LM-GRAALS band (4.5-8 μm) gives approximately $8W/m^2$, explaining the flux difference of the two models at TOA in this band. The bad agreement of the net atmospheric fluxes in the other bands are most probably due to the approximations used by LM-GRAALS in the computations of gaseous optical properties, although the different spectroscopic database used by the models can be an important other source of discrepancy.

In the 2 analysed solar bands (Fig. 3), we can again see a good agreement in the net fluxes profile but a bias in the absolute values. Table 1 shows the percentage difference at surface and at top of atmosphere between the two model's up- and down-welling fluxes. Greatest values can be found in the solar bands and in thermal IR TOA outgoing fluxes.

	TOA Fluxes		Surface Fluxes	
Up Flux	-12.3	-4.6	12.9	0.8
Down Flux	-4.4		-8.8	0.7

Table 1: TOA and Surface Net Fluxes RTX-GRAALS (%)

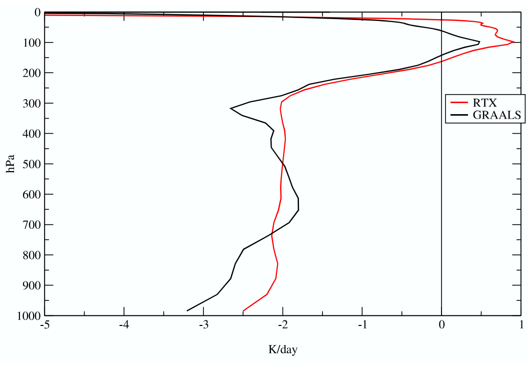

Figure 4: Thermal-IR (104-4.6 μm) Heating Rate; (STD Trop. Atm. Profile)

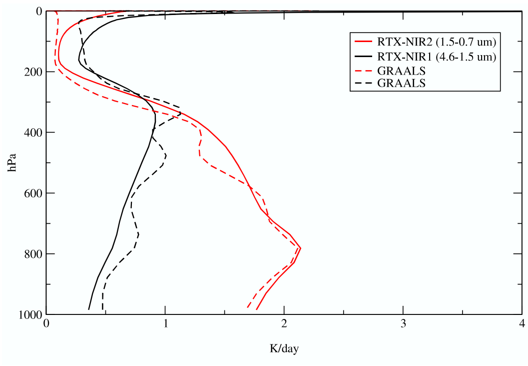

Figure 5: Solar-IR (4.5-0.7 μm) Heating Rate; (STD Trop. Atm. Profile)

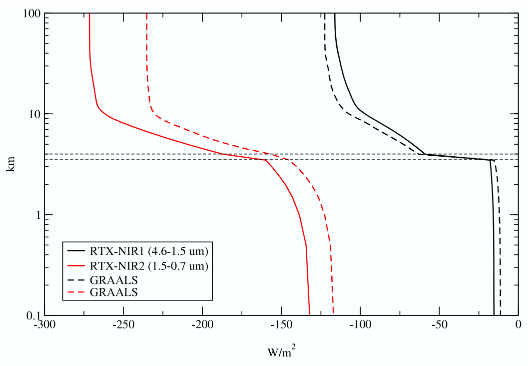

Figure 6: Solar-IR Spectral Net Flux; (Overcast medium-level water cloud: 500m thick; LWC=0.129 g/m^3, re = 5.2 μm; Sun zenith angle = 0°)

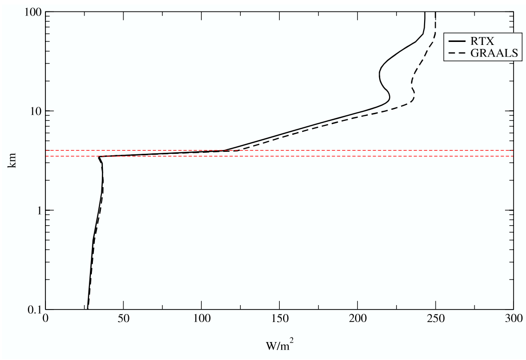

Figure 7: Thermal-IR (104-4.6 μm) Net Flux; (Overcast medium-level water cloud: 500m thick; LWC=0.129 g/m^3, re = 5.2 μm)

The thermal IR heating rate profiles (Fig. 4) show some differences, again due probably to the approximations adopted in LM-GRAALS and to the different spectroscopic database of the two models. We think that upgrading the LM gaseous optical properties can help to improve the computations. In the solar bands, the heating rates (Fig. 5) show good agreement between the models. Nevertheless, work is still in progress in order to extend the comparison at the whole solar spectral range.

In the second scenario, various cloud types have been introduced in the standard tropical profile. Three overcast, homogeneus cloud layers have been generated:

- low-level thick water cloud: 850-715 hPa (1500m thick); LWC=0.5 g/m^3, re = 9.3 μm
- medium-level water cloud: 672-633 hPa (500m thick); LWC=0.129 g/m^3, re = 5.2 μm
- high-level cloud: 266-247 hPa (500m thick); LWC=0.013 g/m^3, re = 4.1 μm

For the medium level clouds, solar net fluxes (Fig. 6, for the low cloud and for different zenith angles a similar situation holds) show the same features emphasized in the clear-sky case; in the thermal IR spectrum (Fig. 7), we can see a fairly good agreement for the net fluxes below the cloud layer, but still disagreement above, as noted in the clear sky case.

Hence it appears that the thermal IR heating rates are in better agreement in cloudy profile than in the clear one (Figs. 8, 9), the differences in the higher layers being unchanged with

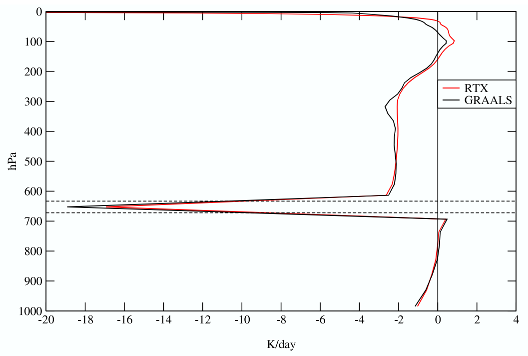

Figure 8: Thermal-IR (104-4.6 μm) Heating Rate; (Overcast medium-level water cloud: 500m thick; LWC=0.129 g/m^3, re = 5.2 μm)

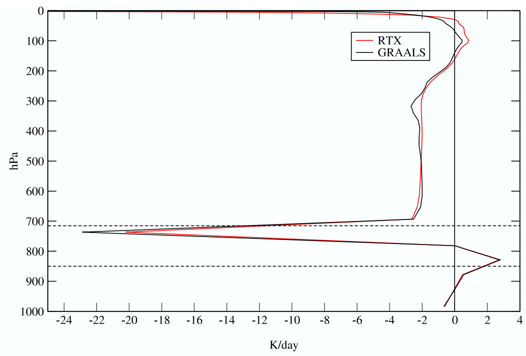

Figure 9: Thermal-IR (104-4.6 μm) Heating Rate; (Overcast low-level water cloud: 1500m thick; LWC=0.5 g/m^3, re = 9.33 μm)

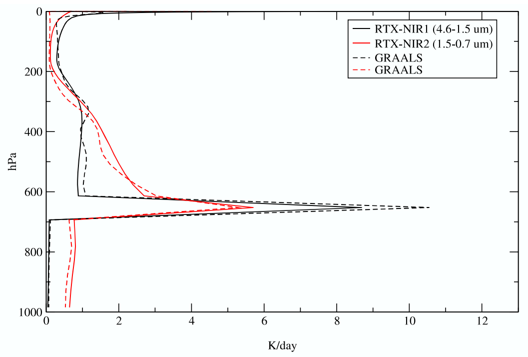

Figure 10: Solar-IR Spectral Heating Rate; (Overcast medium-level water cloud: 500m thick; LWC=0.129 g/m^3, re = 5.2 μm)

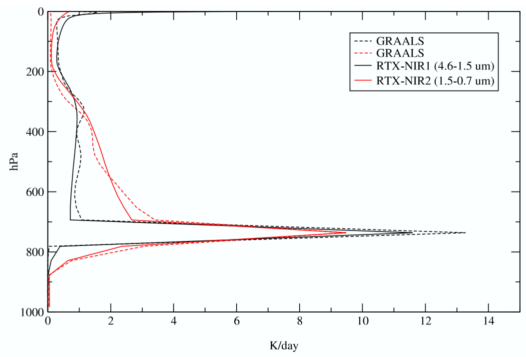

Figure 11: Solar-IR Spectral Heating Rate; (Overcast low-level water cloud: 1500m thick; LWC=0.5 g/m^3, re = 9.33 μm)

respect to the clear sky case. Agreement between the two models can be seen also in the LM solar bands (Figs. 10, 11), the maximum difference between models is noted near the top of the cloud layers, where the maximum heating rate is located. The difference appear to be less evident at shorter wavelengths probably linked to slightly different layer absorption properties, computed approximately by LM_GRAALS and following the exact solution of Mie theory in multiple scattering layers by RTX.

The high, shallow cloud layer has been treated, in first approximation, as water cloud, in spite of the high altitude. It can be seen (Fig. 12) that the thermal IR heating rates show a mean difference of 0.2 K/day to 0.5 K/day below the cloud layer (as in the clear sky case) and a maximum of 1 K/day at the bottom of the cloud layer. The comparison in the solar bands (Fig. 13) is worse as RTX shows strongest heating rate inside the cloud layer. It seems that differences between the models are enhanced by small IWP values.

3 Conclusions and further work

These very first comparisons are showing a reasonably good agreement of the two models in some simple clear and cloudy atmospheric profiles. Some discrepancies in the clear sky profile are linked with the parameterizations adopted by LM-GRAALS and probably also with the old spectroscopic database adopted by the fast radiation code. Actually it appears that the water cloud model can gain fairly good results; nevertheless deeper investigations

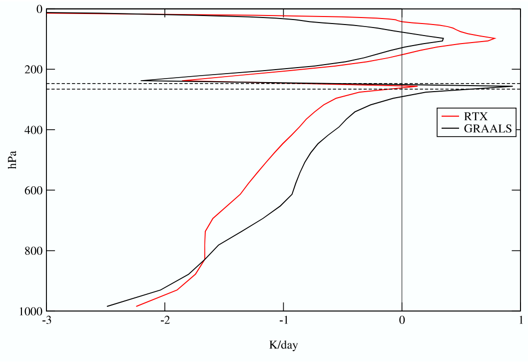

Figure 12: Thermal-IR (104-4.6 μm) Heating Rate; (Overcast high-level water cloud: 500m thick; LWC=0.013 g/m^3, re = 4.1 μm)

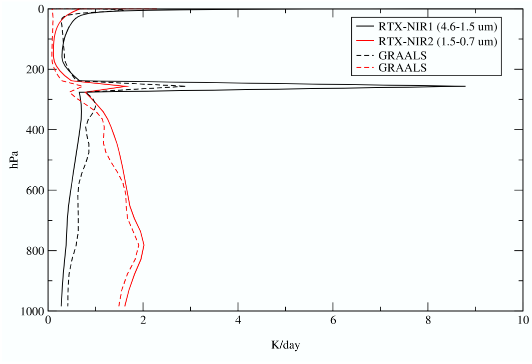

Figure 13: Solar-IR Spectral Heating Rate; (Overcast high-level water cloud: 500m thick; LWC=0.013 g/m^3, re = 4.1 μm)

will be necessary, mostly to clarify the shallow cloud layers optical properties.

This preliminary work is the starting point for further, systematic analysis which will concern the following points:

1. Compute the spectral coefficients for gaseous absorption using the latest release of HITRAN. We are aware of work being done by F. Geleyn on this issue and do not intend to duplicate his effort;
2. Test and eventually improve the parameterization of optical properties of ice clouds, using the most advanced parameterisations for aggregate, columns and possibly hexagonal plates made available to us by the Met Office;
3. Compare the treatment of aerosols in GRAALS and RTX using possibly the most recent version of OPAC (Optical Properties of Aerosols and Clouds) (Hess, Koepke, and Schult, 1998).

References

Slingo, J.M., 1989: A GCM parameterization for the shortwave radiative properties of water clouds. *J. Atmos. Sci.*, 46, pp. 1419-1427.

Slingo, J.M., and Schrecker H. M., 1982: On the shortwave radiative properties of stratiform water clouds. *Quart. J. Roy. Meteor. Soc.*, 108, pp. 407-426.

Stephens, G.L. 1979: Optical properties of eight water cloud types. *CSIRO, Division of Atmospheric Physics*, Technical Paper No. 36, 35 pp.

Ritter B. and Geleyn J.-F. (1992), A comprehensive Radiation Scheme for numerical weather pretiction models with potential applications in climate simulations, Monthly weather review, 120, 303-325

Zdunkowski, W.G., and Korb G.J. (1985), Numerische Methoden zur Loesung der Strahlungsuebertragungsgleichung, PROMET 2/3, 1985, 26-39